First Photometric Study of Two Eclipsing Binary Star Systems: V523 And and V543 And

Oğuz ÖZTÜRK[1,2], and Ahmet ERDEM[1,2]

[1] *Astrophysics Research Centre and Observatory, Çanakkale Onsekiz Mart University, Terzioğlu Kampüsü, TR-17020 Çanakkale, Turkey*
[2] *Department of Physics, Faculty of Arts and Sciences, Çanakkale Onsekiz Mart University, Terzioğlu Kampüsü, TR-17020 Canakkale, Turkey*

Abstract

Detailed photometric analysis of V523 And and V543 And from the Wide Angle Search for Planets survey is presented for the first time. It was found that while V523 And is a detached binary, V543 And is a semi-detached binary star system. The adopted masses and radii for the primary and secondary components are $M_1 = 0.77 \pm 0.08$ M$_\odot$, $R_1 = 0.87 \pm 0.08$ R$_\odot$ and $M_2 = 0.50 \pm 0.12$ M$_\odot$, $R_2 = 0.77 \pm 0.17$ R$_\odot$ for V523 And; and $M_1 = 1.59 \pm 0.16$ M$_\odot$, $R_1 = 1.46 \pm 0.09$ R$_\odot$ and $M_2 = 0.58 \pm 0.17$ M$_\odot$, $R_2 = 1.66 \pm 0.22$ R$_\odot$ for V543 And. Orbital period variations of the systems were analyzed using the O-C method. The O-C change of V523 And is discussed in terms of the magnetic activity cycle of one or both components and light travel time effect (LTTE) due to a third body in the system. Among these mechanisms, LTTE seems to be the most appropriate mechanism to explain the O-C variation of the system since the quadrupole moments of the primary and secondary components (ΔQ) were found to be in the order of 10^{49} g cm^2. The O-C diagram of V543 And shows a downward parabolic trend, which suggests a secular period decrease with a rate of 0.080 ± 0.012 s/year. The parabolic O-C variation of V543 And was interpreted in terms of the non-conservative mass transfer mechanism. According to this scenario, the range of possible values of the mass gain rate ($\dot{M}_1$) of the primary component of V543 And as well as the mass-loss rate ($\dot{M}$) of the system were found to be $10^{-5} - 10^{-11}$ M$_\odot$/year and $10^{-6} - 10^{-8}$ M$_\odot$/year, respectively.

Key words: Binaries: eclipsing; Stars: individual (V523 And; V543 And)

[1] E-mail: oguzozturk@comu.edu.tr

1 Introduction

V523 And (GSC 02290-00900, TYC 2290-900-1, Gaia DR2 369589185726105856, 2MASS J01053795+3649057, V=11.73 mag) and V543 And (GSC 02815-01348, TYC 2815-1348-1, Gaia DR2 319670674926127360, 2MASS J01422531 +3755248, V=10.58 mag) were classified as Algol-type (EA) binary stars by Khruslov (2008) and Kazarovets et al. (2011), respectively. Qian et al. (2018) estimated the effective temperature of the primary star of V523 And to be 5028.53 ± 48.89 K using observations from the Large Sky Area Multi-Object Fibre Spectroscopic Telescope (LAMOST). Although these two systems were observed by several ground-based observational missions, there has been no detailed photometric and/or spectral study on both of the systems so far.

In this study, brief information about the photometric observational missions under which V523 And and V543 And were observed is given in Section 2. In the following section, the precise light curves of V523 And V543 And obtained by the Wide Angle Search for Planets (WASP) (Butters et al. 2010) mission are solved and the geometric parameters of the systems are obtained. Using the *O-C* method, orbital period variation analyses of the systems are given in Section 4. In the last section, the physical parameters of the systems are estimated and the results are discussed.

2 Observations

Photometric observations of V523 And and V543 And were made by following missions: All-Sky Automated Survey for Supernovae (ASAS-SN) (Shappee et al. 2014, Kochanek et al. 2017), Kamogata/Kiso/Kyoto wide-field survey (KWS) (http://kws.cetus-net.org/∼maehara/VSdata.py), Northern Sky Variability Survey (NSVS) (Woźniak et al. 2004) and Wide Angle Search for Planets (WASP) (Butters et al. 2010). Unfiltered observations were carried out by NSVS. While the ASAS-SN observations were performed in V-filters, V and Ic filters were used in the KWS observations. On the other hand, WASP observations were made in broad-band filters (400-700nm). A summary of the photometric observations whose observational data can be retrieved from the literature is given in Table 1.

3 Light Curve Analysis

Light curves of V523 And and V543 And obtained by the WASP Survey were solved for the first time in this study. The WASP observations of V523

Table 1
Brief information about photometric observations of V523 And and V543 And published in the literature.

Survey	Filter	Start-end date of observations (day/month/year)	Number of obs.	Mean obs. error (Mag)
V523 And				
NSVS	Unfiltered	06/06/1999 – 24/02/2000	577	0.025
WASP (Cam105)[1]	Broad band	21/09/2004 – 28/09/2004	4	0.025
WASP (Cam142)[1]	Broad band	07/08/2007 – 17/12/2007	3762	0.016
WASP (Cam145)[1]	Broad band	16/08/2006 – 21/07/2008	975	0.017
WASP (Cam146)[1]	Broad band	30/11/2006 – 23/07/2008	3748	0.012
WASP (Cam147)[1]	Broad band	30/11/2006 – 17/12/2007	3180	0.013
WASP (Cam148)[1]	Broad band	19/07/2008 – 22/07/2008	10	0.023
KWS	V	31/07/2012 – 31/07/2020	1289	0.198
KWS	Ic	07/08/2013 – 31/07/2020	848	0.215
ASAS-SN	V	04/11/2013 – 28/11/2018	262	0.020
V543 And				
NSVS	Unfiltered	06/06/1999 – 09/03/2000	501	0.019
WASP (Cam105)[2]	Broad band	26/06/2004 – 29/09/2004	2334	0.046
WASP (Cam141)[2]	Broad band	20/08/2007 – 17/12/2007	3738	0.028
WASP (Cam147)[2]	Broad band	20/08/2007 – 23/07/2008	3106	0.020
WASP (Cam148)[2]	Broad band	21/08/2006 – 03/01/2007	3044	0.055
KWS	V	05/12/2010 – 27/09/2020	843	0.069
KWS	Ic	07/08/2013 – 27/09/2020	649	0.114
ASAS-SN	V	10/12/2013 – 28/11/2018	256	0.020

Notes:
[1] Observations with observational error larger than 0.030 mag not included.
[2] Observations with observational error larger than 0.055 mag not included.

And were made with cameras 105, 142, 145, 146 and 148 (see Table 1). Brief information about the WASP observations with observational error values less than 0.030 mag are given in Table 1. The most precise observations of this system were carried out with camera 146. Using camera 146, 3748 observations were taken with error values between 0.007 mag and 0.030 mag (see Table 1). We selected 1216 observations from these observations, with errors less than 0.009 mag, to be able to solve the WASP light curve accurately.

The WASP observations of V543 And were made with cameras 105, 141, 147 and 148 (see Table 1). We give brief information about the WASP observations of the system with an observational error smaller than 0.055 mag in Table 1. The most precise CCD observations of this system were carried out with camera 147. Using camera 147, 3748 observations were taken with error values from 0.003 mag to 0.055 mag (see Table 1). From these observations, we selected 562 observations of V543 And with an error smaller than 0.005 mag in order to determine the reliable geometric parameters of the system.

Before starting the analysis, the effective temperatures of the primary stars were determined. In the case of V523 And, we took the effective temperature of the primary component from Qian et al. (2018) to be $T_1 = 5029 \pm 49$ K, which was estimated from spectroscopic observations of the system. On the other hand, the temperature of the primary component of V523 And is given as 5055K in Gaia DR2. Therefore, the tempertaure value given by Qian et al. (2018) is compatible with that of the value given in Gaia DR2 (Gaia Collaboration 2018) within error limits.

Since no spectroscopic observations have been carried out for V543 And, we estimated the effective temperature of the primary component using the method given by Tunçel Güçtekin et al. (2016). In this method, the effective temperature of the primary is estimated from the intrinsic color index, $(B-V)_0$, of the binary system. Firstly, we determined the V band total absorption of V543 And located at galactic latitude b, $A_{(\infty,V)}(b)$ from Schlafly & Finkbeiner (2011), using the NASA Extragalactic Database (http://ned.ipac.caltech.edu /forms/calculator.html). Following this, the interstellar absorption for the system's distance d, $A_d(b)$ was calculated using the equation given by Bahcall & Soneira (1980) below, where H is the scale height and its value was assumed to be 125 pc, according to Marshall et al. (2006), and the distance of the system was calculated using its Gaia DR2 (Gaia Collaboration 2018) parallax:

$$A_{d,V}(b) = A_{\infty,V}(b)\left[1 - \exp\left(-\frac{|d\sin b|}{H}\right)\right] \quad (1)$$

The color excess of the system was then estimated from $E_d(B-V) = A_{d,V}(b)/3.1$. The intrinsic color index of V543 And was found to be 0.38 ± 0.07 mag using $(B-V)_0 = (B-V) - E_d(B-V)$. Finally, the effective temperature of the primary component was estimated to be 6880 ± 200 K, according to Drilling & Landolt (2000)'s color index-effective temperature calibration for main sequence stars. However, the temperature of the primary component of V543 And is given as 7244 K in Gaia DR2. Therefore, the light curve solution of the system was carried out separately for both temperature values.

After determining the effective temperatures of the primary components of V523 And and V543 And, the light curves were phased using the ephemerides obtained in the orbital period analysis (see Section 4). Wilson-Devinney (W-D) code (Wilson & Devinney 1971, Wilson 2012) was used for the light curve analysis. Effective wavelengths of the observations were assumed to be 550 nm since the WASP mission was performed in wide-band filters ($400 - 700$ nm). The bolometric gravity-darkening exponents of the components were taken to be 1.0 for a radiative atmosphere ($T > 7200$ K) from von Zeipel (1924) and 0.32 for a convective atmosphere ($T < 7200$ K) from Lucy (1967) . Also, the bolometric albedos of the components were fixed to 1.0 and 0.5 for the radiative and convective atmospheres, respectively, following Ruciński (1969).

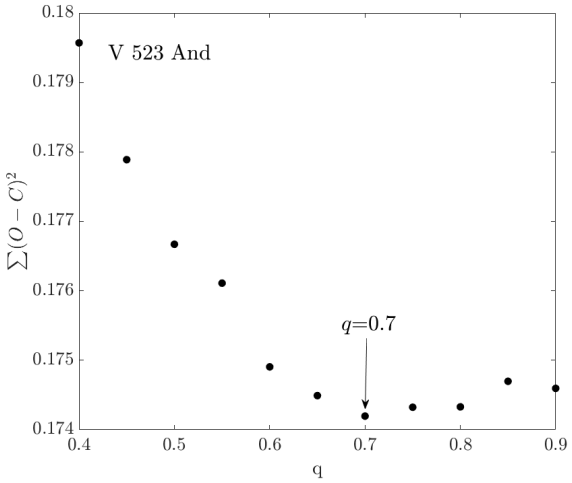

Figure 1. Sum of squared residuals ($\Sigma(O-C)^2$) versus related mass ratio (q) values obtained under cold spot assumption of V523 And.

The third light contributions for both systems were disregarded. We assumed that the components of the systems were rotating synchronously in circular orbits, ($e = 0$).

Light curve analysis of V523 And was performed in mode 2 (detached configuration). Phase shift (ϕ), orbital inclination (i), effective temperature of the secondary component (T_2), dimensionless surface gravities of the primary and secondary components (Ω_1, Ω_2), mass ratio (q) and luminosity of the primary component (L_1) were chosen to be free parameters during the iterations. The light curve of V523 And is asymmetric, i.e., the primary maxima of the light curve is higher than the second maxima (see Figure 2). This asymmetry may arise from cold or hot spot activity on the more massive primary component.

Before starting the light curve solutions, the q-search method was carried out separately for the hot and cold spot assumptions to obtain the photometric mass ratio of V523 And, since the spectroscopic mass ratio of the system has not been published in the literature. All parameters mentioned above, except the mass ratio, were set as free parameters during the q-search procedure. During the q-search, the sum of the squared residuals $\Sigma(O-C)^2$ value obtained from the hot spot assumption was found to be larger than that of the value obtained from the cold spot assumption. Therefore, the light curve solution of V523 And was performed under the cold spot assumption. Figure 1 shows the sum of the squared residuals $\Sigma(O-C)^2$ of the light curve models for a cold spot assumption with respect to the related mass ratio values.

The minimum $\Sigma(O-C)^2$ values were achieved at $q = 0.7$ for the cold spot assumption. We also set the following as free parameters of the cold spot; colatitude and longitude, radius, and dimensionless fractional temperature

factor (T_{spot}/T_1). Initial values of the mass ratio parameter were set to $q = 0.7$ for the cold spot model. The best model parameters obtained from the light curve solution are given in Table 2.

Table 2
Parameters obtained from best W-D model fits to WASP light curves of V523 And and V543 And.

	V523 And	V543 And
Parameter	Value	Value
ϕ	0.0012 ± 0.0001	-0.0005 ± 0.0001
i(deg.)	81.6 ± 1.3	77.3 ± 1.0
T_1(K)	5029	7244
T_2(K)	4830 ± 160	4287 ± 115
$q(= M_2/M_1)$	0.650 ± 0.092	0.369 ± 0.069
Ω_1	4.148 ± 0.017	3.972 ± 0.023
Ω_2	3.759 ± 0.016	2.613
r_1(vol.)	0.292 ± 0.005	0.282 ± 0.001
r_2(vol.)	0.258 ± 0.006	0.321 ± 0.002
L_1	7.696 ± 0.025	11.361 ± 0.036
L_2	4.784	1.053
Spot parameters		
Co-latitude (deg.)	90 ± 12	-
Longitude (deg.)	108 ± 21	-
Spot radius (deg.)	15 ± 3	-
T_{spot}/T_1	0.90 ± 0.08	-
χ^2_{red}	14.965	24.347

The chi-squared (χ^2) values of the model fits were calculated using the equation below given by Bevington (1969), where $l_{i,O}$ and $l_{i,C}$ are the observed and calculated light levels at a given phase, respectively, and Δl_i is an error estimate for the measured values of $l_{i,O}$.

$$\chi^2 = \sum_i \frac{(l_{i,O} - l_{i,C})}{\Delta l_i^2} \tag{2}$$

Next, we calculated the reduced chi-squared value of the model fits from $\chi^2_{red} = \chi^2/\nu$, where ν is the number of degrees of freedom of the data set. The χ^2_{red} value obtained from the cold spot model was 14.965 (see Table 2).

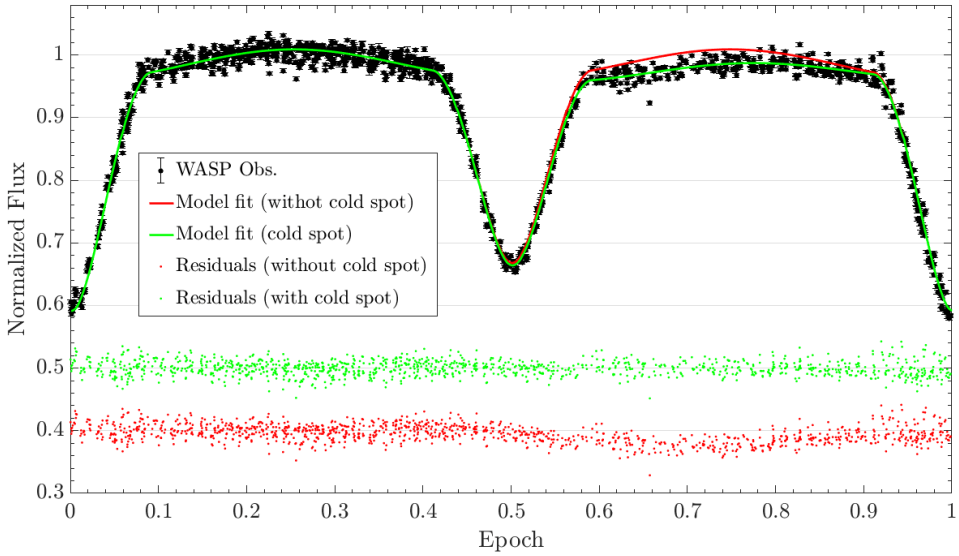

Figure 2. Observed light curve of V523 And from WASP survey. Best theoretical fit obtained under cold spot assumption is shown by solid green line. Solid red line corresponds to light curve model fit without star-spot assumption. Green and red filled-dots correspond to residuals obtained from cold spot and without spot models, respectively.

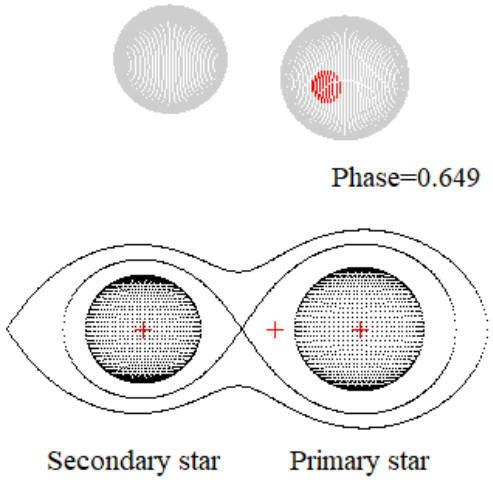

Figure 3. Roche geometry of V523 And obtained from light curve analysis. Red region in upper part illustrates cold spot on primary component.

The theoretical fit obtained from the cold spot model together with the observed light curve is shown in Figure 2.

The Roche geometry of V523 And obtained from the derived light curve parameters under the cold spot model is given in Figure 3. According to the solution, while the primary component of V523 And fills 77 per cent of its Roche lobe, the secondary component fills 85 per cent of its Roche lobe.

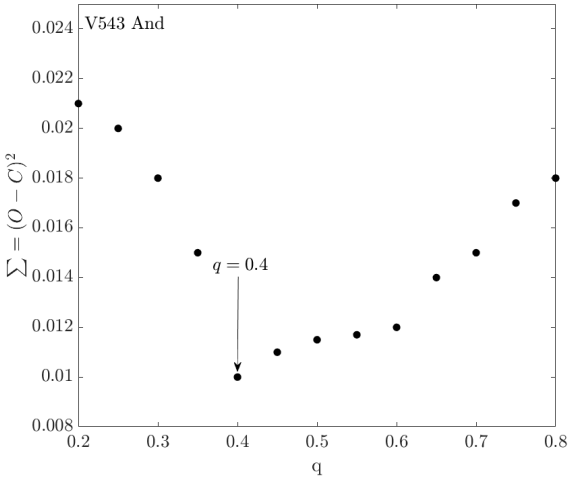

Figure 4. Sum of squared residuals ($\Sigma(O-C)^2$) versus related mass ratio (q) values of V543 And for $T_1 = 7244$ K.

Light curve analysis of V543 And was started in mode 2 (detached configuration). After a few iterations, we noted that the secondary component fills its critical Roche lobe. Thus, we continued the light curve solution in mode 5, a semi-detached configuration. In this solution, phase shift (ϕ), orbital inclination (i), effective temperature of the secondary component (T_2), dimensionless surface gravity of the primary component (Ω_1), mass ratio (q) and luminosity of the primary component (L_1) were chosen as the free parameters during the iterations.

As in the case of V523 And, the q-search method was carried out to obtain the photometric mass ratio of V543 And since the spectroscopic mass ratio of the system has not been published in the literature. The q-search procedure was performed separately for $T_1 = 6880$ K, which was estimated using the method of Tunçel Güçtekin et al. (2016), and $T_1 = 7244$ K, which is given in Gaia DR2. All parameters mentioned above except the mass ratio were set as free parameters during the q-search procedure. The minimum value of $\Sigma(O-C)^2$ was achieved at $q = 0.4$ for both of the temperature values.

As an example of the least $\Sigma(O-C)^2$ reached, Figure 4 shows the sum of the squared residuals $\Sigma(O-C)^2$ of the light curve models with respect to the related mass ratio values for $T_1 = 7244$K. Therefore, the initial value of the mass ratio was set to $q = 0.4$ for the light curve solution. The reduced chi-squared value (χ^2_{red}) of the model fit was calculated to be 25.534 for $T_1 = 6880$ K and 24.347 for $T_1 = 7244$ K. The minimum value of χ^2_{red} was reached in the solution for $T_1 = 7244$ K. In addition to this, in Gaia DR2, the temperatures of the stars, with effective temperatures between 3000 K and 10000 K, were estimated to be within the typical 324 K uncertainty from the two distance-independent G_{BP} – G (330 – 680 nm) and G - G_{RP} (630 – 1050 nm) colors

(Gaia Collaboration 2018, Andrae et al. 2018). Due to this , only the light curve solution parameters obtained at the $T_1 = 7244$ K temperature value are given in Table 2.

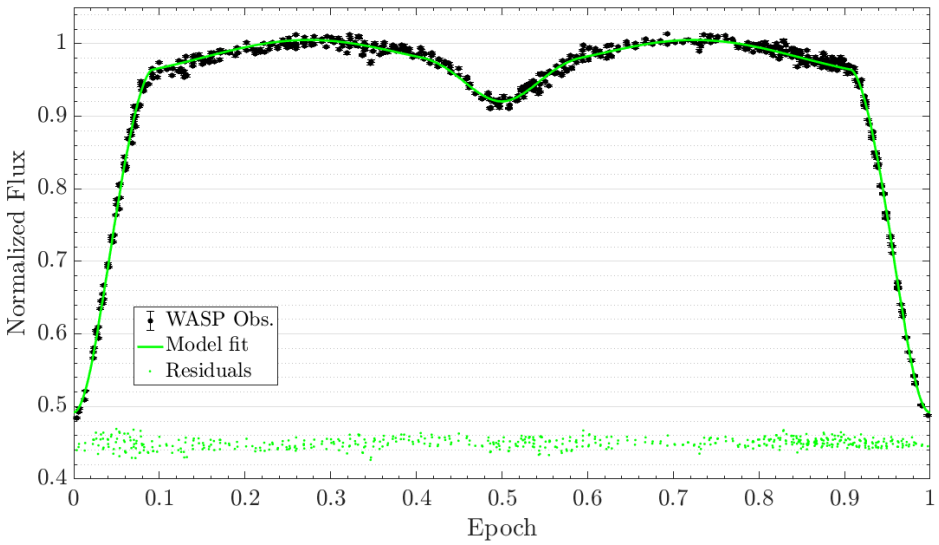

Figure 5. Observed light curve of V543 And from WASP survey. Best theoretical fit obtained from light curve analysis for $T_1 = 7244$ K is illustrated by solid green line. Green-filled points correspond to residuals.

The best theoretical fit obtained from the light curve analyses, together with the observed light curve, is shown in Figure 5. The Roche geometry of V543 And obtained from the best light curve solution is given in Figure 6. According to our solution of the light curve of V543 And, while the secondary component completely fills its Roche lobe, the primary component fills only 66 per cent

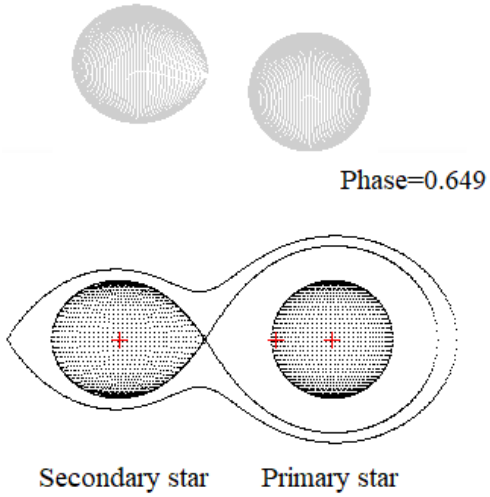

Figure 6. Roche geometry of V543 And obtained from best light curve solution.

of its Roche lobe.

4 Orbital Period Analysis

Orbital period variation analyses of V523 And and V543 And were performed for the first time in this study. The *O-C* method was used in the analyses using a MATLAB code given by Zasche et al. (2009).

Eclipse timings of V523 And published in the literature are as follows: 1 CCD timing by Khruslov (2008), 3 CCD timings by Hoňková et al. (2013), 2 photoelectric (Pe) timings by Hübscher & Lehmann (2013), 1 CCD timing by Nelson (2014), 3 CCD timings by Juryšek et al. (2017), 1 Pe timing by Hübscher (2017), and 1 CCD timing by Nelson (2018). One additional CCD eclipse time is also given in the O-C Gateway Database (http://var2.astro.cz/ocgate/). As a result, the total number of eclipse timings of V523 And published in the literature so far is 13.

In this study, a total of 64 CCD timings were calculated from the WASP observations using the Kwee-van Woerden method (Kwee & van Woerden 1956). Since very few observation points were collected per night by the ASAS-SN, NSVS and KWS surveys, a method given in the study of Zasche et al. (2014) was used in order to estimate the timings from these surveys. Although the primary and secondary eclipse phases are evident in the ASAS-SN and NSVS light curves, the eclipses are not obvious due to wide scattering in the KWS light curves. Therefore, we were not able to calculate precise timings from the KWS observations.

In the method given by Zasche et al. (2014), firstly, all light curves observed within the scope of the relevant observation project were divided into 1-year regions. Afterwards, each data set was phased using the linear light element below, where the conjunction time $T_0 = 2455799.56943$ HJD and the orbital period $P = 0.52854$ days of V523 And were taken from Hoňková et al. (2013) and Khruslov (2008), respectively.

$$C_{1,\mathrm{V523\ And}}(\mathrm{Min\ I/Min\ II}) = \mathrm{HJD}\ 2455799.56943 + 0^{\mathrm{d}}.52854 \times E \qquad (3)$$

After this, the light curve fit to each data set was acquired using Wilson-Devinney software (W-D) (Wilson & Devinney 1971, Wilson 2012). In this step, while the phase shift parameter was adjusted to be a free parameter, the values of the remaining parameters, which were taken from the best light curve fit obtained in the previous section, were kept constant. Finally, the theoretical minima for each data set were derived (see Zasche et al. 2014).

In this way, 11 eclipse timings were calculated from the ASAS-SN and NSVS observations. Therefore, the total number of timings obtained in this study together with the times published in the literature reached 88. The eclipse timing data used in the *O-C* analysis of the V523 And system covers a period of approximately 19 years between October, 1999 and June, 2018.

The timings of V543 And published in the literature are as follows: 1 CCD timing by Khruslov (2008), 3 CCD timings by Hoňková et al. (2013), 1 Pe timing by Hübscher (2015), 1 Pe timing by Hübscher (2017), 2 Pe timings by Pagel (2018) and 1 Pe timing by Pagel (2020). In total, 9 eclipse timings of V543 And have been published in the literature. We also calculated 42 CCD timings from WASP observations of V543 And using the Kwee-van Woerden method.

Since only a few observational points were taken per night in the ASAS-SN, NSVS and KWS observations, the eclipse timings in these observation projects were calculated using Zasche et al. (2014)'s method. The light curve data sets were phased using the following light element, where T_0 = 2454344.65264 HJD and P = 0.9264 days are the conjunction time obtained in this study from WASP observations and the orbital period taken from Khruslov (2008), respectively.

$$C_{1,\mathrm{V543\ And}}(\mathrm{Min\ I/Min\ II}) = \mathrm{HJD}\ 2454344.65264 + 0^{\mathrm{d}}.9264 \times E \tag{4}$$

We theoretically calculated 5, 6 and 11 timings from the ASAS-SN, NSVS and KWS observations, respectively, using the method given by Zasche et al. (2014). Therefore, the total number of eclipse times of V543 And obtained in this study, together with the times published in the literature, is 73. The timing data used in the *O-C* analysis of V543 And covers almost 21 years from October, 1999 to August, 2020.

The eclipse timings data of V523 And and V543 And are given in the Appendix.

The *O-C* diagram of V523 And is given in Figure 7. As seen in the diagram, the *O-C* shows an upward parabolic trend. Under the assumption of a parabolic *O-C* variation, the quadratic ephemeris, which includes the orbital period (P) of the system, conjunction time (T_0) and quadratic parameter, was found as below:

$$\begin{aligned} C_{2,\mathrm{V523\ And}}(\mathrm{Min\ I/Min\ II}) = \mathrm{HJD}\ 2455799.56732(25) + 0^{\mathrm{d}}.5285397(1) \times E \\ +1^{\mathrm{d}}.59(10) \times 10^{-10} \times E^2 \end{aligned} \tag{5}$$

The quadratic term of V523 And was found to be $1.59(\pm 0.10) \times 10^{-10}$ days.

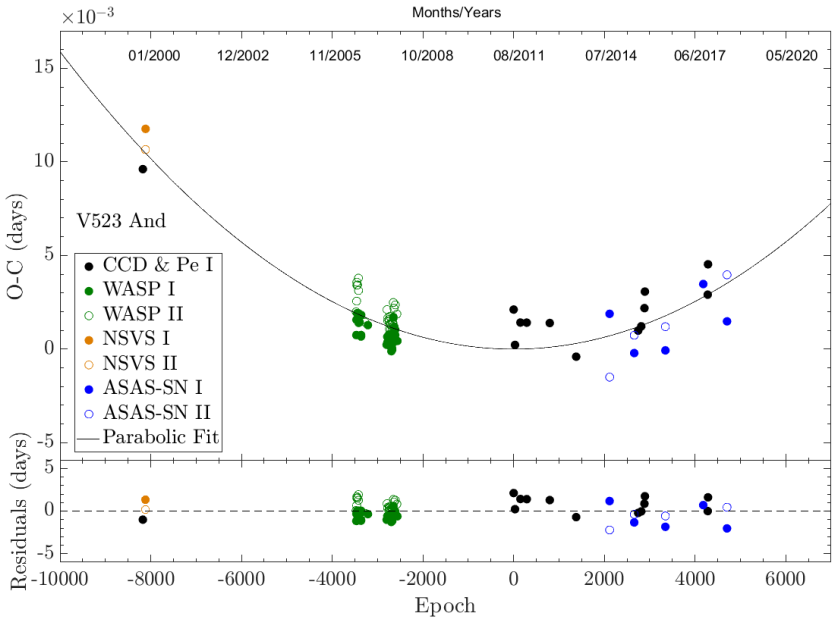

Figure 7. *O-C* diagram of V523 And. Best parabolic fit to *O-C* dataset is shown with solid black line. Residuals from parabolic fit are shown in bottom part of diagram.

According to the quadratic term obtained, we found that the orbital period of the system is secularly increasing with a slow rate of 0.019(±0.003) seconds per year.

This observed orbital period increase may be due to a non-conservative mass transfer mechanism from the secondary component to the primary component, as discussed in the next section for V543 And. In this case, the mass transfer rate must be greater than the rate of mass lost from the system (Tout & Hall 1991, Erdem & Öztürk 2014). For mass transfer from the secondary component to the primary component to occur, the secondary component must have filled its critical Roche lobe. However, it was concluded from the light curve solution of V523 And that it is a detached binary star system (see Section 3). Therefore, the orbital period increase seen in V523 And could not be explained by the mass transfer mechanism.

On the other hand, the upward parabolic *O-C* variation may be a part of sinusoidal *O-C* variation due to the magnetic activity cycle of one or both components (see Applegate 1992). In order to examine this anomaly, a sinusoidal fit was made on the *O-C* diagram of V523 And using the least squares method. The amplitude ($A^{'}$) and period ($P^{'}$) of the sinusoidal *O-C* variation were obtained as 0.0032(±0.0005) days and 19.43(±3.59) years, respectively, and the sum of square residuals ($\Sigma(O-C)^2$) obtained from the fit is 0.00086 days^2. In this case, the rate of period variation ($\Delta P/P$) can be determined

using the following equation given by Applegate (1992).

$$\frac{\Delta P}{P} = 2\pi \frac{A^{'}}{P^{'}} \tag{6}$$

The rate of period variation of V523 And due to possible magnetic activity is calculated to be $\Delta P/P = 2.87 \times 10^{-6}$ using the equation above. In order to produce such a hypothetical cyclic *O-C* variation, the change that has to occur in the quadrupole moment of each component can be calculated using the equation below, given by Lanza & Rodonó (1999).

$$\frac{\Delta P}{P} = -9 \frac{\Delta Q}{M_{1,2} A^2} \tag{7}$$

The quadrupole moments of the primary and secondary components were found to be $\Delta Q_1 = 2.10 \times 10^{49}$ g cm^2 and $\Delta Q_2 = 1.36 \times 10^{49}$ g cm^2, respectively, from Eq. 7 using the M_1, M_2 and A values given in Table 4. As is known, in close binary stars, the quadrupole moment values of the components with effective magnetic activity vary between 10^{51} g cm^2 and 10^{52} g cm^2 (Lanza & Rodonó 1999). Since our ΔQ_1 and ΔQ_2 values are considerably smaller than the acceptable values, the possible sinusoidal cycle in the *O-C* diagram of the system could not be explained either by the magnetic activity cycle of the components.

Another possible cause of cyclic *O-C* variation may be the light travel time effect (LTTE) due to a third body which is physically bound to the system. In order to examine this situation, the following LTTE equation given by Irwin (1959) was fitted to the *O-C* diagram of the system.

$$\Delta t = \frac{a_{12} \sin i_{12}}{c} \left\{ \frac{1 - e_{12}^2}{1 + e_{12} \cos \nu_{12}} \sin(\nu_{12} + \omega_{12}) + e_{12} \cos \omega_{12} \right\} \tag{8}$$

where Δt is the time advance/delay due to LTTE, c is the speed of light, and a_{12}, i_{12}, e_{12} and ω_{12} are the semi-major axis, inclination, eccentricity and longitude of the periastron of the absolute orbit of the centre of mass of the eclipsing binary around the three-body system, respectively. ν_{12} is the true anomaly of the position of the eclipsing binary's mass center on this orbit and includes T_{12} and P_{12} (the unseen/hidden parameters of Eq. 8, where T_{12} is the epoch of the passage at the periastron of the eclipsing binary's mass center along its orbit, and P_{12} is its orbital period).

The LTTE analysis was performed using a MATLAB code given by Zasche et al. (2009). The best theoretical fit made to the *O-C* diagram and the residuals obtained from the fit are shown in Figure 8, and the derived parameters are

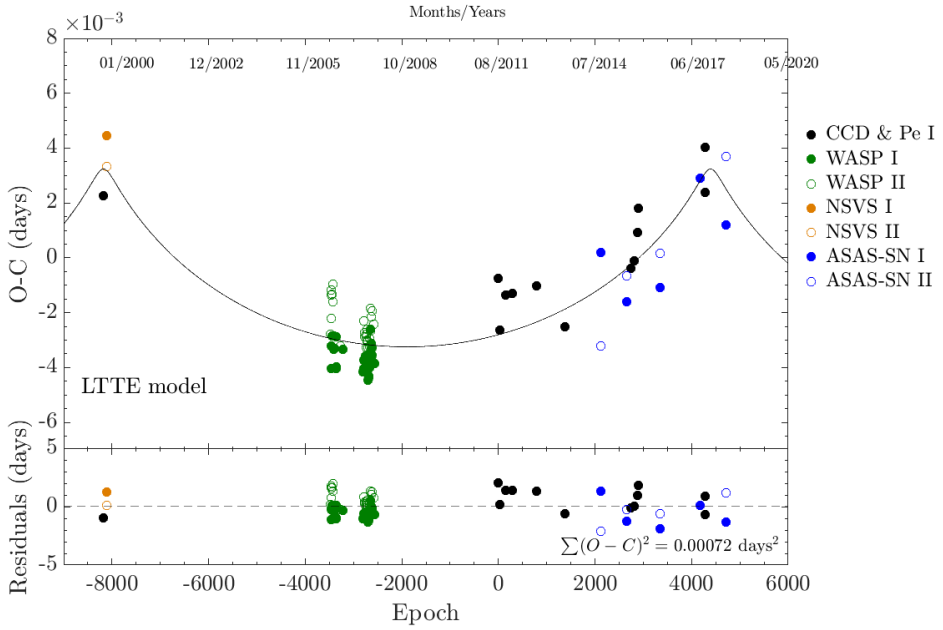

Figure 8. LTTE representation (solid black line) of O-C variation of V523 And, and residuals from the best-fit curve.

Table 3
Parameters obtained from LTTE analysis of V523 And.

Parameters	Value
T_0 (HJD)	2455799.5701 ± 0.0003
P (day)	0.5285391 ± 0.0000001
$A^{'}$ (day)	0.0032 ± 0.0001
$a_{12} \sin i_{12}$ (AU)	0.56 ± 0.12
e_{12}	0.83 ± 0.15
ω_{12} (deg)	90 ± 15
P_{12} (years)	18.2 ± 1.6
$f(M_3)$ ($M_\odot$)	0.00053 ± 0.00007
M_3 ($M_\odot$) for $i_{12} = 30^0$	0.21 ± 0.07
M_3 ($M_\odot$) for $i_{12} = 60^0$	0.12 ± 0.05
M_3 ($M_\odot$) for $i_{12} = 90^0$	0.10 ± 0.03

given in Table 3. The sum of square residuals ($\Sigma(O-C)^2$) from the best fit is 0.00072 days^2, which is lower than that of the sinusoidal fit. According to the parameters given in Table 3, V523 And orbits around the triple system's center of mass in an eccentric orbit ($e_{12} = 0.83(\pm 0.15)$) with a period of $P_{12} = 18.2(\pm 1.6)$ years. The projected distance of the center of mass of V523

And to the center of mass of the three- body system was estimated to be $a_{12}\sin i_{12} = 0.56(\pm0.12)$ AU. Using the P_{12} and $a_{12}\sin i_{12}$ values, the mass function of the third body was found to be $f(M_3) = 0.00053(\pm0.00007)$ $M_\odot$. More discussion on the LTTE effect is presented in the final section.

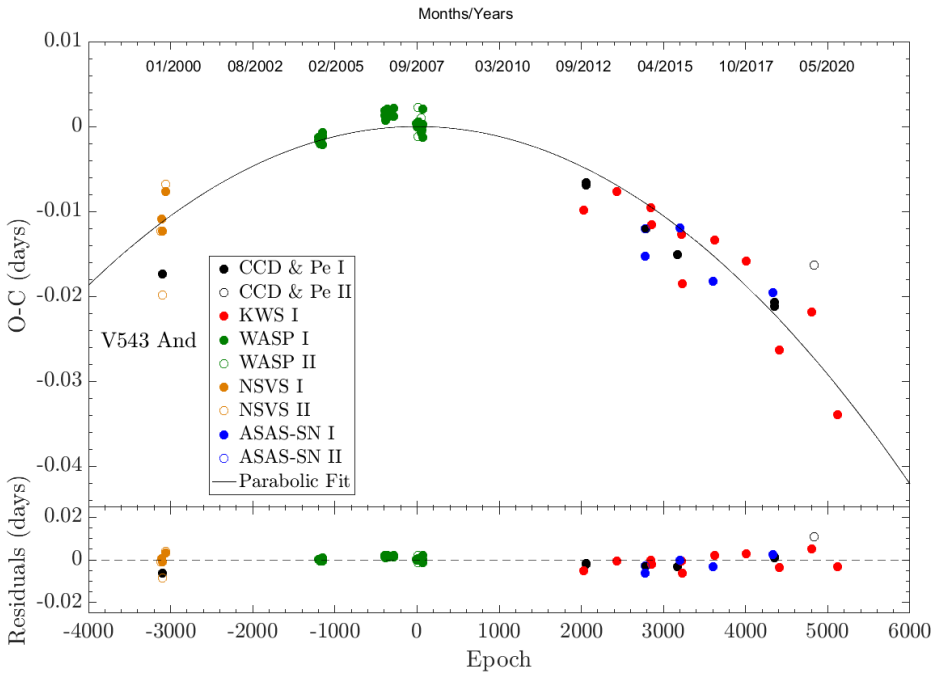

Figure 9. Same as Figure 7 but for V543 And.

The *O-C* diagram of V543 And is given in Figure 9. The *O-C* shows a downward parabolic change. Therefore, under the assumption of parabolic *O-C* variation, the quadratic ephemeris of V543 And was found to be as below:

$$C_{2,\mathrm{V543\ And}}(\mathrm{Min\ I/Min\ II}) = \mathrm{HJD}\ 2454344.6527(13) + 0^{\mathrm{d}}.9263708(6) \times E$$
$$-11^{\mathrm{d}}.68(63) \times 10^{-10} \times E^2 \qquad (9)$$

According to the quadratic ephemeris, the quadratic term of V543 And is $-11.68(\pm0.63) \times 10^{-10}$ days. This value suggests that the orbital period of the system is decreasing at a rate of $0.080(\pm12)$ seconds per year. Since it was understood in the previous section that the secondary component of this system completely filled its Roche lobe, the *O-C* change in the system can be interpreted in terms of mass transfer from the less massive component to the more massive component, which is examined in detail in the next section.

5 Results and Discussion

Since there are no published radial velocity measurements of either system, we estimated their absolute parameters, as given in Table 4. The masses of the primary components were estimated using the calibrations of the color index, effective temperature, mass and spectral type for main-sequence stars given by Drilling & Landolt (2000). We assumed a 10 per cent error in the estimated masses of the primary components in order to estimate the errors of the remaining parameters given in Table 4. The mass of the secondary component of V523 And and V543 And were calculated from the photometric mass ratios given in Table 2. The semi-major axes (A) were derived from Kepler's third law. Lastly, the bolometric magnitudes (M_{bol}) and surface gravity ($\log g$) values were estimated using the solar values ($T_{eff} = 5771.8 \pm 0.7$ K, $M_{bol} = 4.7554 \pm 0.0004$ mag, and $g = 27423.2 \pm 7.9$ cm/s^2) given by Pecaut & Mamajek (2013).

Table 4
Estimated absolute parameters of V523 And and V543 And.

	V523 And		V543 And	
	Primary star	Secondary star	Primary star	Secondary star
(A) ($R_\odot$)	2.98±0.06		5.17 ± 0.10	
$M(M_\odot)$	0.77 ± 0.08	0.50 ± 0.12	1.59 ± 0.16	0.58 ± 0.17
$R(R_\odot)$	0.87 ± 0.08	0.77 ± 0.17	1.46 ± 0.09	1.66 ± 0.22
$\log g$ (cgs)	4.45 ± 0.11	4.37 ± 0.10	4.31 ± 0.10	3.76 ± 0.09
M_{bol} (mag)	5.66 ± 0.68	6.10 ± 0.79	2.95 ± 0.35	4.95 ± 0.64

In the previous section, we argued that the O-C variation of V523 And could not be interpreted in terms of the mass transfer mechanism between the components or the magnetic activity cycles of the components. In order to explain the O-C change of the system, LTTE was considered in the same section. According to the masses of the primary and secondary components of V523 And given in Table 4, the mass of the hypothetical third body was found to be 0.21(±0.07) $M_\odot$, 0.12(±0.05) $M_\odot$, and 0.10(±0.03) $M_\odot$ for $i_{12} = 30^0$,$i_{12} = 60^0$ and $i_{12} = 90^0$, respectively. If the third body is coplanar with the binary star system ($i_{12} = i = 81^0.6 \pm 1^0.3$, see Table 2), then the mass and semi-major axis of its orbit around the center of the mass of the three- body system is derived to be 0.10(±0.04) $M_\odot$ and 7(±1) AU. According to Allen's tables for main-sequence stars (Drilling & Landolt 2000), if we assume that the third body is a main-sequence star then it should be a dwarf of late-M spectral type. The light contribution of the third body to the total light of the system was estimated to be $\sim 0.04\%$ using the mass- luminosity relation of $L \sim M^{3.9}$ given by İbanoğlu et al. (2006). Therefore, the light contribution from the

third body is too small to be observed photometrically.

On the other hand, we calculated the semi-amplitude of the changes in the systemic velocity (K_{RV}) accompanied by LTTE to be approximately 1.65 km/s, which can be detected by future high precision radial velocity measurements of the system, using the equation below given by Mayer (1990).

$$K_{RV} = \frac{2\pi}{P_{12}} \frac{a_{12} \sin i_{12}}{\sqrt{1 + e_{12}^2}} \tag{10}$$

In conclusion, the most plausible scenario to explain the *O-C* change of the V523 And system is the LTTE effect due to the third body. However, in order to confirm the existence of this third body, high-precision radial velocity measurements of the system are needed. Further precise photometric observations, especially minima times, are also paramount in determining the long-term *O-C* variation.

We found that the secondary component of V543 And completely fills its Roche lobe. It is known that a fraction of the mass can be transferred to the more massive primary component when the less massive secondary fills its Roche lobe. In this case, the orbital period of the binary star system may show a periodic increase. In addition, a partial fraction of the mass can also be lost due to the magnetic braking effect of stellar winds, which give rise to a decrease in the orbital period of the binary system. Therefore, we considered the combined effect of mass transfer and mass loss from the system, i.e. a non-conservative mass transfer mechanism, to interpret the orbital period change of V543 And. We used the equation given by Erdem & Öztürk (2014) in order to calculate the rate of mass transfer from the secondary component to primary component and the rate of mass loss from the system. The relation between the rate of orbital period change and the rate of mass transfer and loss in semi-detached binaries is given below by Erdem & Öztürk (2014):

$$\frac{\dot{P}}{P} = \left\{ 2 \left\{ \frac{R_A}{A} \right\}^2 \frac{M_1 + M_2}{M_1 M_2} - \frac{2}{M_1 + M_2} \right\} \dot{M} + \frac{3\,(M_1 - M_2)}{M_1 + M_2} \dot{M}_1 \tag{11}$$

where $\dot{P}$and $\dot{M}_1$ are the rate of orbital period change and the rate of transferred mass from the secondary to primary component, respectively. R_A is the Alfvén radius, inside which matter lost from the system is co-rotating with the mass losing secondary star. $\dot{M}$represents the rate of mass loss from the system and is defined as below:

$$\dot{M} \leq (1 - \beta)\, \dot{M}_2 = \frac{(\beta - 1)}{\beta} \dot{M}_1 \tag{12}$$

where $\dot{M}_2$ is the mass loss rate of the secondary component and $\beta = -\frac{\dot{M}_1}{\dot{M}_2}$ is the mass-loss parameter giving the fraction of mass lost by the secondary component that is accreted by the primary component.

The critical value of the mass-loss parameter (β_{cri}) can be derived from Eqs. 11 and 12. The β_{cri} value of V543 And was found to be 0.936 under the assumption that the R_A is $10R_2$ (see Tout & Hall 1991).

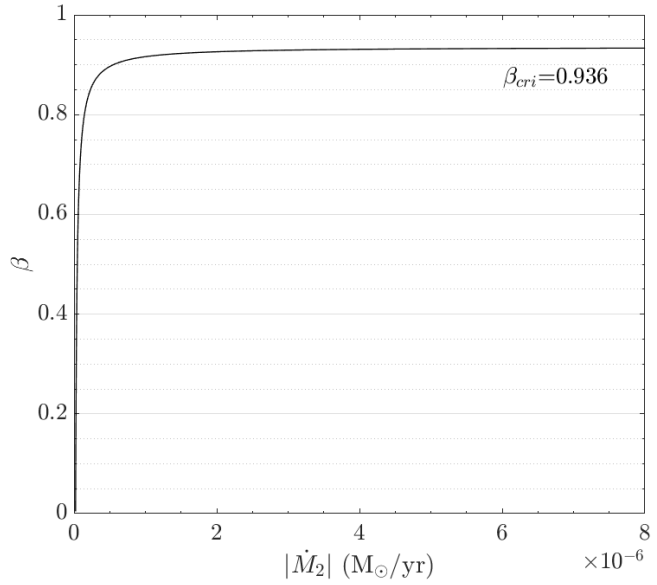

Figure 10. Change of mass-loss parameter (β) with respect to mass-loss rate ($\dot{M}_2$) of secondary component of V543 And.

If the mass-loss parameter is smaller than its critical value, then the mass-loss from the system via stellar wind is the dominant mechanism and the orbital period of the binary system subsequently decreases (see Erdem & Öztürk 2014). Using Eqs. 11 and 12 for $0 < \beta < 0.936$, we found the range of possible values of the mass gain rate ($\dot{M}_1$) of the primary component of V543 And and the mass-loss rate ($\dot{M}$) of the system to be 10^{-5}-10^{-11} $M_\odot$/year and 10^{-6}-10^{-8} $M_\odot$/year, respectively. The β-$\dot{M}_2$ diagram of V543 And is given in Figure 10.

In this study, a detailed appraisal of eclipsing binary systems V523 And and V543 And was given for the first time. High-resolution spectroscopic observations together with more precise photometric observations of these systems are required in order to estimate their absolute parameters more reliably, to understand the nature of the long-term *O-C* variation of V523 And, and to understand the mass flow properties and evolutionary status of the component stars of V543 And.

Acknowledgements

This study made use of the SIMBAD and NASA Astrophysics Data System Bibliographic Services as well as data from the WASP, ASAS-SN, KWS and NSVS surveys. We would like to thank the anonymous referee who provided valuable comments for improving the manuscript. We also thank Mr. G.H. Lee for checking the English.

References

Applegate, J.H., 1992. A Mechanism for Orbital Period Modulation in Close Binaries. ApJ 385, 621-629. https://doi.org/10.1086/170967

Andrae, R., Fouesneau, M., Creevey, O. et al. 2018, Gaia Data Release 2. First stellar parameters from Apsis. A&A 616, id.A8. https://doi.org/10.1051/0004-6361/201732516

Bahcall, J. N., Soneira, R. M., 1980, The universe at faint magnitudes. I. Models for the Galaxy and the predicted star counts. ApJS 44, 73-110. https://doi.org/10.1086/190685

Bevington P. R., 1969, Data Reduction and Error Analysis for the Physical Sciences. McGraw-Hill, New York. https://ui.adsabs.harvard.edu/abs/1969drea.book.....B/abstract

Butters, O. W., West, R. G., Anderson, D. R. et al. 2010, The first WASP public data release. A&A 520, id.L10. https://doi.org/10.1051/0004-6361/201015655

Drilling, J. S., Landolt, A. U., 2000, Allen's astrophysical quantities, 4th ed. Edited by Arthur N. Cox. ISBN: 0-387-98746-0. Publisher: New York: AIP Press; Springer, p.381. https://ui.adsabs.harvard.edu/abs/2000asqu.book..381D/abstract

Erdem, A., Öztürk, O., 2014, Non-conservative mass transfers in Algols. MNRAS 441 (2), 1166-1176. https://doi.org/10.1093/mnras/stu630

Gaia Collaboration, 2018, Gaia Data Release 2. Summary of the contents and survey properties. A&A 616, id.A1. https://doi.org/10.1051/0004-6361/201833051

Hübscher, J., Lehmann, P. B., 2013, BAV-Results of observations - Photoelectric Minima of Selected Eclipsing Binaries and Maxima of Pulsating Stars. IBVS 6070 (1). https://ui.adsabs.harvard.edu/abs/2013IBVS.6070....1H/abstract

Hübscher, J., 2015, BAV-Results of observations - Photoelectric Minima of Selected Eclipsing Binaries and Maxima of Pulsating Stars. IBVS 6152 (1). https://ui.adsabs.harvard.edu/abs/2015IBVS.6152....1H/abstract

Hübscher, J., 2017, BAV-Results of observations - Photoelectric Minima of

Selected Eclipsing Binaries and Maxima of Pulsating Stars. IBVS 6196 (1). https://doi.org/10.22444/IBVS.6196
Hoňková, K., Juryšek, J., Lehký, M., et al. 2013, B.R.N.O. Contributions #38 Times of minima. OEJV 160, 1-174. https://ui.adsabs.harvard.edu/abs/2013OEJV..160....1H/abstract
Irwin, J. B., 1959, Standard light-time curves. AJ 64, 149-155. https://doi.org/10.1086/107913
İbanoğlu, C. , Soydugan, F. , Soydugan, E. , Dervişoğlu, A, 2006, Angular momentum evolution of Algol binaries. MNRAS 373 (1), 435-448. https://doi.org/10.1111/j.1365-2966.2006.11052.x
Juryšek, J., Hoňková, K., Šmelcer, L., et al. 2017, B.R.N.O. Contributions 40 Times of minima. OEJV 179, 1-145. https://ui.adsabs.harvard.edu/abs/2017OEJV..179....1J/abstract
Kazarovets, E. V., Samus, N. N., Durlevich, O. V. et al. 2011, The 80th Name-List of Variable Stars. Part I - RA 0h to 6h. IBVS 5969, 1-21. https://konkoly.hu/pub/ibvs/5901/5969.pdf
Khruslov, A. V., 2008, New Algol-Type Eclipsing Binaries III. PZP 8 (41), 1-2. http://www.astronet.ru/db/varstars/msg/eid/PZP-08-0041
Kochanek, C. S., Shappee, B. J., Stanek, K. Z., et al. 2017, The All-Sky Automated Survey for Supernovae (ASAS-SN) Light Curve Server v1.0. PASP 129 (980), pp. 104502. https://doi.org/10.1088/1538-3873/aa80d9
Kwee, K. K., van Woerden, H., 1956,A method for computing accurately the epoch of minimum of an eclipsing variable. BAN 12, 327-330. https://ui.adsabs.harvard.edu/abs/1956BAN....12..327K/abstract
Lanza, A. F., Rodonó ,M. 1999, Orbital period modulation and quadrupole moment changes in magnetically active close binaries. A&A 349, 887-897. https://ui.adsabs.harvard.edu/abs/1999A%26A...349..887L/abstract
Lucy, L. B., 1967, Gravity-Darkening for Stars with Convective Envelopes. ZA 65, 89-92. https://ui.adsabs.harvard.edu/abs/1967ZA.....65...89L/abstract
Marshall, D.J., Robin, A.C., Reylé, C., et al. 2006, Modelling the Galactic interstellar extinction distribution in three dimensions. A%A 453 (2), 635-651. https://doi.org/10.1051/0004-6361:20053842
Mayer, P., 1990, Eclipsing Binaries with Light-time Effect. BAICz 41, 231-236. https://ui.adsabs.harvard.edu/abs/1990BAICz..41..231M/abstract
Nelson, R. H., 2014, CCD Minima for Selected Eclipsing Binaries in 2013. IBVS 6092 (1). https://ui.adsabs.harvard.edu/abs/2014IBVS.6092....1N/abstract
Nelson, R. H., 2018, CCD Minima for Selected Eclipsing Binaries in 2017. IBVS 6234 (1). https://doi.org/10.22444/IBVS.6234
Pagel, L., 2018, BAV-Results of observations - Photoelectric Minima/Maxima of Selected Eclipsing Binaries and Maxima/Minima of Pulsating Stars. BAVJ 249. https://www.bav-astro.eu/images/Up_Journal/BAVJ031_R3_BAVM249.pdf
Pagel, L., 2020, BAV-Results of observations - Photoelectric Minima/Maxima of Selected Eclipsing Binaries and Max-

ima/Minima of Pulsating Stars. BAVJ 251. https://www.bav-astro.eu/images/Up_Journal/BAVJ033_BAVM251_R1.pdf

Pecaut, M. J., Mamajek, E. E., 2013, Intrinsic Colors, Temperatures, and Bolometric Corrections of Pre-main-sequence Stars. ApJS 208 (1), id. 9. https://doi.org/10.1088/0067-0049/208/1/9

Qian, S. -B., Zhang, J., He, J. -J. et al. 2018, Physical Properties and Evolutionary States of EA-type Eclipsing Binaries Observed by LAMOST. ApJS 235 (1), id.5. https://doi.org/10.3847/1538-4365/aaa601

Ruciński S. M., 1969, The Proximity Effects in Close Binary Systems. II. The Bolometric Reflection Effect for Stars with Deep Convective Envelopes. AcA 19, 245-255. https://ui.adsabs.harvard.edu/abs/1969AcA....19..245R/abstract

Schlafly, E. F., Finkbeiner, D. P., 2011, Measuring Reddening with Sloan Digital Sky Survey Stellar Spectra and Recalibrating SFD. ApJ 737 (2), id.103. https://doi.org/10.1088/0004-637X/737/2/103

Shappee, B. J., Prieto, J. L., Grupe, D. et al. 2014, The Man behind the Curtain: X-Rays Drive the UV through NIR Variability in the 2013 Active Galactic Nucleus Outburst in NGC 2617. ApJ 788 (1), id.48. https://doi.org/10.1088/0004-637X/788/1/48

Tout, C.A. , Hall, D.S. , 1991, Wind driven mass transfer in interacting binary systems. MNRAS 253, 9-18. https://doi.org/10.1093/mnras/253.1.9

Tunçel Güçtekin, S., Bilir, S., Karaali, S., Ak, S., Ak, T., Bostancı, Z. F., 2016, Metallicity calibration and photometric parallax estimation: I. UBV photometry. Ap&SS 361 (6), id.186. https://doi.org/10.1007/s10509-016-2776-2

von Zeipel, H. 1924, The radiative equilibrium of a rotating system of gaseous masses. MNRAS 84, 665-683. https://doi.org/10.1093/mnras/84.9.665

Wilson, R. E., Devinney, E. J., 1971, Realization of Accurate Close-Binary Light Curves: Application to MR Cygni. ApJ 166, 605-619. https://doi.org/10.1086/150986

Wilson, R. E., 2012, Spotted Star Light Curves with Enhanced Precision. AJ 144 (3), id.73. https://doi.org/10.1088/0004-6256/144/3/73

Woźniak, P. R., Vestrand, W. T., Akerlof, C. W., et al. 2004,Northern Sky Variability Survey: Public Data Release. AJ 127 (4), 2436-2449. https://doi.org/10.1086/382719

Zasche, P. , Liakos, A. , Niarchos, P. , et al. 2009, Period changes in six contact binaries: WZ And, V803 Aql, DF Hya, PY Lyr, FZ Ori, and AH Tau. NewA 14 (2), 121-128. https://doi.org/10.1016/j.newast.2008.06.002

Zasche, P., Wolf, M., Vraštil, J., et al. 2014, Apsidal motion and a light curve solution for eighteen SMC eccentric eclipsing binaries. A&A 572 , id.A71. https://doi.org/10.1051/0004-6361/201424273

Highlights

- Light curves of V523 And and V543 And obtained by the WASP Survey were solved for the first time in this study .
- We concluded that that while V523 And is a detached binary, V543 And is a semi-detached binary star system.
- Orbital period analyses of V523 And and V543 And were performed and results were discussed for the first time in this study.
- Absolute parameters of V523 And and V543 And were estimated.